Phase Transformation in the Surface Region of Zirconia Detected by UV Raman Spectroscopy

ARTICLE *in* THE JOURNAL OF PHYSICAL CHEMISTRY B · AUGUST 2001

Impact Factor: 3.3 · DOI: 10.1021/jp010526l

Phase Transformation in the Surface Region of Zirconia Detected by UV Raman Spectroscopy

Meijun Li, Zhaochi Feng, Guang Xiong, Pinliang Ying, Qin Xin, and Can Li*

State Key Laboratory of Catalysis, Dalian Institute of Chemical Physics, Chinese Academy of Sciences, P.O. Box 110, Dalian 116023, China

Received: February 9, 2001; In Final Form: June 18, 2001

The phase transformation of zirconia from tetragonal to monoclinic is characterized by UV Raman spectroscopy, visible Raman spectroscopy, and XRD. Electronic absorption of ZrO_2 in the UV region makes UV Raman spectroscopy more sensitive at the surface region than XRD or visible Raman spectroscopy. Zirconia changes from the tetragonal phase to the monoclinic phase with calcination temperatures elevated and monoclinic phase is always detected first by UV Raman spectroscopy for the samples calcined at lower temperatures than that by XRD and visible Raman spectroscopy. When the phase of zirconia changes from tetragonal to monoclinic, the slight changes of the phase at very beginning can be detected by UV Raman spectroscopy. UV Raman spectra clearly indicate that the phase transition takes place initially at the surface regions. It is found that the phase change from tetragonal to monoclinic is significantly retarded when amorphous $Zr(OH)_4$ was agglomerated to bigger particles and the particle agglomeration of amorphous zirconium hydroxide is beneficial to the stabilization of t-ZrO_2 phase.

Introduction

Recent research progress in zirconia has greatly enhanced the prospects for applying this material as catalyst, catalyst support, ceramic, engineering gemstone, fuel cell, pigment, automotive gas sensor, etc.[1−6] Its varied chemical properties including reducing, oxidizing, and acidic and basic properties make zirconia an attractive catalyst or catalyst support for a number of reactions.[1,5,7−9] For example, zirconia impregnated with sulfate ions has superacidic behavior and shows high activity for hydrocarbon isomerization and methanol conversion to hydrocarbons.[10−13]

Zirconia exhibits three different phases: monoclinic (m-ZrO_2), which is stable below 1170 °C; tetragonal (t-ZrO_2), which is stable between 1170 °C and 2370 °C; and cubic (c-ZrO_2), stable from 2370 °C to its melting temperature at 2680 °C. Besides m-ZrO_2, metastable t-ZrO_2 can be stable at room temperature.[2,14,15] Metastable t-ZrO_2 can be obtained by the thermal treatment of suitable starting materials (zirconium salt, zirconium alkoxides, or zirconium hydroxide).[1,2,15,16] Stabilized tetragonal zirconia is considered an important structure for ceramics because of its excellent mechanical properties such as fracture toughness, strength, and hardness. However, a phase transformation from the metastable tetragonal (t) phase to the monoclinic (m) phase of crystalline ZrO_2 prevents its applications from a broader temperature ranges. Many studies have addressed the factors that affect the phase transformation of tetragonal zirconia, such as the amount of stabilizer,[17,18] the pH values of precipitation in the synthesis,[2] the grain size of the tetragonal powder,[19,20] water vapor in its crystalline growth,[21] and intrinsic defects such as vacancies in the anionic sublattice.[22,23] However, these investigations provided the information mainly on the bulk of ZrO_2.

Ultraviolet Raman spectroscopy (UVRS) is a powerful tool for the study of catalysts and other solids.[24−29] Raman scattering comes usually from both the surface and the bulk of a solid sample, but the signal from the bulk is attenuated when the sample strongly absorbs the excitation laser light and scattering light. Therefore, UV Raman spectroscopy is more sensitive to the surface region of zirconia because zirconia shows a strong absorbance in the UV region. In this work, we have studied the phase transformation of zirconia using UVRS together with visible Raman spectroscopy and XRD. It is found that the results from UV Raman spectroscopy are different compared with those from XRD and visible Raman spectroscopy, particularly when the tetragonal phase begins to change into the monoclinic phase. On the basis of the results of UV Raman spectroscopy, visible Raman spectroscopy, and XRD, it is concluded that the phase transformation of zirconia takes place initially at surface regions, then develops into the bulk.

Experimental Section

$Zr(OH)_4$ was obtained by adding aqueous ammonia slowly to the solution of zirconium oxychloride at room temperature under stirring until the pH value of the solution reached ∼10. The precipitate thus obtained was washed thoroughly with distilled water until chloride ions were not detected, and then was dried at 110 °C for 12 h. The dried precipitate sample, in the forms of powder pressed and unpressed, was calcined at different temperatures for 2 h. The pressure for making the pressed pellet was about 5 MPa. UV, VIS Raman spectra, and XRD patterns were recorded at room temperature for the calcined powder unpressed and pressed samples.

UV Raman spectra were recorded on a homemade UV Raman spectrograph, which has four main parts: an UV cw laser, a Spex 1877d triplemate spectrograph, a CCD detector, and an optical collection system. The 244-nm line from Innova 300 FRED was used as the excitation source. The laser power of the 244-nm line at the samples was below 2.0 mw. Visible

* Author to whom correspondence should be addressed. Tel: 8-411-4671991, ext. 728, 726. Fax: +86-411-4694447. E-mail: canli@ms.dicp.ac.cn. Homepage: http://www.canli.dicp.ac.cn.

10.1021/jp010526l CCC: $20.00
Published on Web 08/08/2001

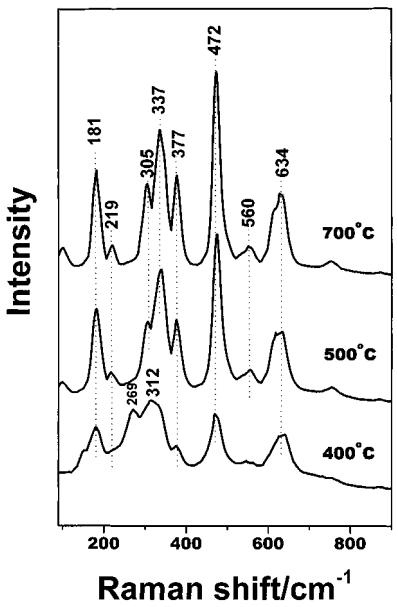

Figure 1. UV Raman spectra of unpressed powder $Zr(OH)_4$ calcined at 400 °C, 500 °C, and 700 °C.

Raman spectra were recorded on a Jobin-Yvon U1000 scanning double monochromator with the spectrum resolution of 4 cm^{-1} using a laser at 532 nm line as the excitation source. The Raman signal was collected with a 90°-geometry.

UV−Vis diffuse reflectance spectra were recorded on a JASCO V-550 UV−Vis Spectrophotometer. XRD patterns were collected on a Rigaku Rotaflex (RU-200B) powder diffractometry equipped with a Cu target and a Ni filter.

Results and Discussion

Figure 1 displays the UV Raman spectra of unpressed powder samples calcined at different temperatures. It can be seen in the Raman spectrum that the major bands are at 181, 269, 312, 472, and 634 cm^{-1} with weak bands at 149, 377, and 556 cm^{-1} for the zirconia sample calcined at 400 °C. The Raman bands at 149, 269, and 312 cm^{-1} are assigned to the Raman-active modes for the tetragonal phase of ZrO_2, B_{1g} at 149 cm^{-1}, E_g at 269 cm^{-1}, and B_{1g} at 312 cm^{-1}. The bands at 181, 337, 472, 556, and 634 cm^{-1} are assigned to the Raman-active modes for the monoclinic phase of ZrO_2, A_g at 181 cm^{-1}, B_g at 377 cm^{-1}, A_g at 472 cm^{-1}, A_g at 558 cm^{-1}, and A_g at 634 cm^{-1}.[30] The band at 269 cm^{-1} appears only for t-ZrO_2 and the band at 181 cm^{-1} appears only for m-ZrO_2. In addition, there are two main differences in the Raman spectra between the monoclinic phase and the tetragonal phase of zirconia, i.e., the band at 472 cm^{-1} is stronger than the band at 634 cm^{-1} for the monoclinic phase and the reverse for the tetragonal phase, and there are some small bands between 472 and 634 cm^{-1} for the monoclinic phase, but these weak bands are absent for the tetragonal phase. Obviously, the UV Raman spectrum of the sample calcined at 400 °C is due to mixed phases of t-ZrO_2 and m-ZrO_2.

After the sample was calcined at 500 °C, the Raman bands due to t-ZrO_2 (149, 269, and 312 cm^{-1}) disappear as shown in Figure 1, while the bands of m-ZrO_2 (181, 337, 472, 560, and 634 cm^{-1}) develop. In addition, some Raman bands appear at 219, 305, and 337 cm^{-1}, which are assigned to the Raman-active modes for m-ZrO_2, B_g at 220 cm^{-1}, A_g at 305 cm^{-1}, and B_g at 337.[30] The Raman spectrum of the sample calcined at 500 °C shows the bands mainly attributed to m-ZrO_2. The Raman bands of the monoclinic phase increase in intensity further after the sample was calcined at 700 °C (see Figure 1).

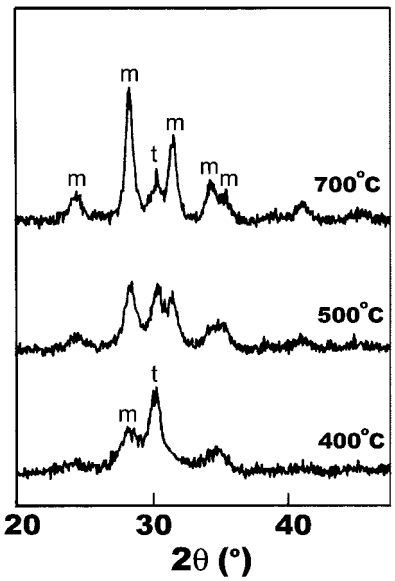

Figure 2. XRD patterns of unpressed powder $Zr(OH)_4$ calcined at 400 °C, 500 °C, and 700 °C.

Figure 2 shows the XRD patterns of unpressed samples calcined at different temperatures. The "t" and "m" in the figure denote the tetragonal and monoclinic phases, respectively. After the sample was calcined at 400 °C, the diffraction peaks of the tetragonal phase are predominant, and the peaks of the monoclinic phase are relatively weak. Besides, small portion of ZrO_2 may be still remained as amorphous phase after the sample was calcined at 400 °C because the XRD peaks are somewhat broad. This means that the zirconia is mainly in the tetragonal phase. However, from UV Raman spectra, it is seen that the zirconia is a mixture of phases m-ZrO_2 and t-ZrO_2. The diffraction peaks of t-ZrO_2 decline and the peak intensities of m-ZrO_2 increase after the sample was calcined at 500 °C. But the XRD peaks of t-ZrO_2 are still very strong, indicating that the t-ZrO_2 phase is still a big fraction in the zirconia. On the contrary, the UV Raman spectra (Figure 1) suggest that zirconia is nearly all in the monoclinic phase. After the sample was calcined at 700 °C, it can be observed that the diffraction peaks of m-ZrO_2 are predominant, and the diffraction peaks of t-ZrO_2 become weak. The results of XRD suggest that some t-ZrO_2 phase still exist even after the sample was calcined at 700 °C.

From the comparison between Figure 1 and Figure 2, it can be seen that there are distinct differences between the results from UV Raman spectroscopy and XRD. According to UV Raman spectra, the Raman bands due to the mixed phases (t-ZrO_2 and m-ZrO_2) are observed for the zirconia calcined at 400 °C, and only the Raman bands of m-ZrO_2 are detected after the sample was calcined at 500 °C. But the results from XRD indicate that t-ZrO_2 is the dominant phase after the calcination at 400 °C and it can be detected even after the calcination at 700 °C.

Figure 3 shows the visible Raman spectra of unpressed zirconia samples calcined at different temperatures. It is observed that Raman bands of t-ZrO_2 are dominant in the spectrum after the sample was calcined at 400 °C, because the characteristic bands of t-ZrO_2 at 149, 269, and 313 cm^{-1} are relatively strong, and the band at 640 cm^{-1} is stronger than the band at 469 cm^{-1}. After the sample was calcined at 500 °C, the intensities of the bands at 178, 189, and 379 cm^{-1} attributed to m-ZrO_2 increase somewhat. The band at 469 cm^{-1} is slightly stronger than the band at 640 cm^{-1}. This suggests that the portion of m-ZrO_2 phase in zirconia is increased, but there is

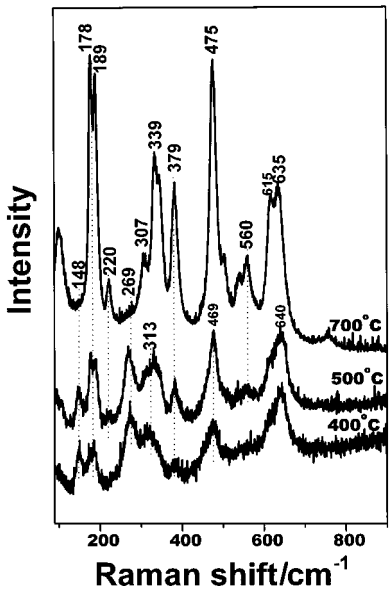

Figure 3. Visible Raman spectra of unpressed powder $Zr(OH)_4$ calcined at 400 °C, 500 °C, and 700 °C.

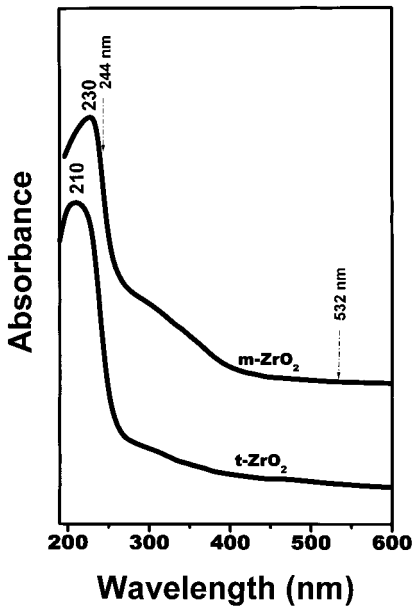

Figure 4. UV−Visible diffuse reflectance spectra of zirconia.

still very much t-ZrO_2. For the sample calcined at 700 °C, the Raman bands at 178, 189, 220, 307, 339, 379, and 635 cm^{-1} due to monoclinic phase become considerably stronger. Very interestingly, the results from visible Raman spectroscopy are in good agreement with the results from XRD (Figure 2).

Generally speaking, Raman scattering comes from both the surface and the bulk of a solid sample. But the signal from the bulk is attenuated when the sample strongly absorbs the excitation laser light and the scattering light, and the Raman spectra then contain more signal from the surface top region than the bulk of a sample. In particular, most transition metal oxides strongly absorb UV laser light, so UV Raman spectroscopy is more sensitive to the surface region than to the bulk for these samples. Visible Raman spectroscopy gives the information from both the bulk and the surface of a sample because there is usually no electronic absorption in the visible region for most samples.

UV−Visible diffuse reflectance spectra of zirconia show two broad bands centered at 210 and 230 nm (Figure 4). The laser line at 244 nm is near the electronic absorption of ZrO_2. Accordingly, the phase transformation in the surface region could be detected selectively by UV Raman spectroscopy. In contrast, it is hard to separate the information of the surface phase from the bulk phase of zirconia using visible Raman spectroscopy, because there is no electronic absorption in the visible region for zirconia.

The m-ZrO_2 phase is detected by UV Raman spectroscopy when the samples are calcined at relatively lower temperatures compared with XRD and visible Raman spectroscopy. The fact that the results from UV Raman spectra disagree with those from XRD and visible Raman can be interpreted only as that the phase transformation of zirconia starts from the surface region and then progresses to the bulk. The initial change of the phase at the surface region can be sensitively detected by UV Raman spectroscopy but not by XRD and visible Raman spectroscopy.

The influence of mechanical treatment on the phase transformation from t-ZrO_2 to m-ZrO_2 was also investigated using UV Raman spectroscopy and XRD. Figure 5 displays the UV Raman spectra of pressed samples calcined at different temperatures. After the pressed sample was calcined at 400 °C, the

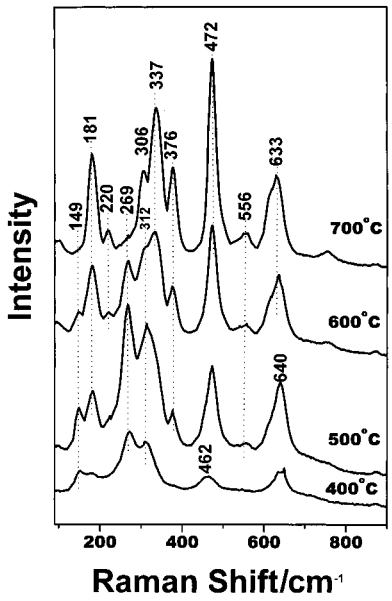

Figure 5. UV Raman spectra of pressed $Zr(OH)_4$ calcined at 400 °C, 500 °C, 600 °C, and 700 °C.

UV Raman spectrum gives strong bands at 149, 269, 312, 462, and 640 cm^{-1}. The band at 640 cm^{-1} is stronger than the band at 462 cm^{-1}. These features are readily attributed to the t-ZrO_2 phase, but a tiny band at 181 cm^{-1} due to m-ZrO_2 phase can be observed. As the calcination temperature was increased to 500 °C, the bands at 149, 269, and 312 cm^{-1} attributed to t-ZrO_2 phase become slightly stronger, and the weak bands at 181, 270, and 556 cm^{-1} attributed to the m-ZrO_2 phase begin to appear. After the sample was calcined at 600 °C, the intensities of the bands at 149, 269, and 312 cm^{-1} decrease, while those of bands at 181, 376, and 556 cm^{-1} increase. The typical Raman bands at 220 and 337 cm^{-1}, attributed to m-ZrO_2, become evident. The Raman spectrum of the pressed sample calcined at 700 °C gives the strong bands of m-ZrO_2 at 181, 220, 306, 337, 376, 472, and 634 cm^{-1}, and the bands of t-ZrO_2 disappear.

Figure 6 shows the XRD patterns of the pressed samples calcined at different temperatures, to compare with the UV Raman spectra (Figure 5). It is found that only the tetragonal phase is present after the pressed sample was calcined at 400

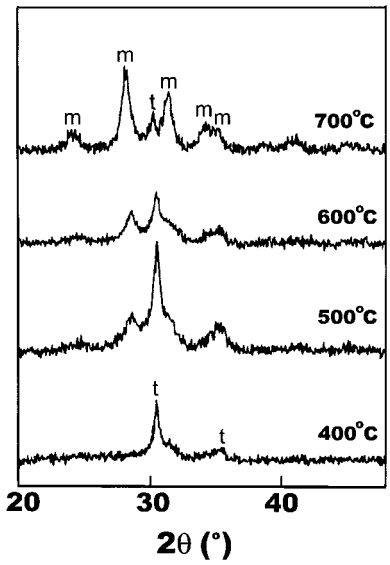

Figure 6. XRD patterns of pressed $Zr(OH)_4$ calcined at 400 °C, 500 °C, 600 °C, and 700 °C.

°C (Figure 6). But in the UV Raman spectra (Figure 5), a relatively weak band of m-ZrO_2 at 181 cm^{-1} is observed. As the sample was calcined at 500 °C, some weak diffraction peaks of m-ZrO_2 appear, but zirconia is still mainly in the tetragonal phase. From UV Raman spectra (Figure 5), the zirconia is a mixture of phases of t-ZrO_2 and m-ZrO_2. As the calcination temperature was increased to 600 °C, the diffraction peaks of t-ZrO_2 decline and the peak intensities of m-ZrO_2 increase, however, the XRD peak of t-ZrO_2 is still quite strong. On the contrary, from UV Raman spectra (Figure 5), it can be observed that the m-ZrO_2 phase forms the major portion of the zirconia. When the sample was calcined at 700 °C, the XRD peaks of m-ZrO_2 are predominant and the peaks of t-ZrO_2 become weak, while the UV Raman bands of t-ZrO_2 disappear (Figure 5). From UV Raman spectra (Figure 5) and XRD (Figure 6) of the pressed samples, on one hand, it is found that the m-ZrO_2 phase can be first detected by UV Raman spectroscopy when the samples were calcined at temperatures relatively lower than that by XRD. On the other hand, the t-ZrO_2 phase disappear at relatively lower temperatures deduced from UV Raman spectra than from XRD. This obvious discrepancy again suggests that the phase transformation from t-ZrO_2 to m-ZrO_2 take place initially at surface region.

Comparing Figure 1 with Figure 5, differences can be found for the phase changes between the unpressed and pressed powder samples. After the samples were calcined at 400 °C, the UV Raman bands at 181, 269, 312, 377, 472, and 634 cm^{-1} due to the mixture with nearly equally amount of t-ZrO_2 and m-ZrO_2 are detected for the unpressed powder sample (Figure 1), but, for the pressed sample, the bands of t-ZrO_2 at 149, 269, 312, 462, and 640 cm^{-1} are predominant (Figure 5). After the samples were calcined at 500 °C, mainly the Raman bands of m-ZrO_2 are observed for the unpressed sample (Figure 1), while the bands attributed to t-ZrO_2 are still dominant for the pressed sample (Figure 5). The UV Raman bands of t-ZrO_2 can be observed even after the pressed sample was calcined at 600 °C (Figure 5).

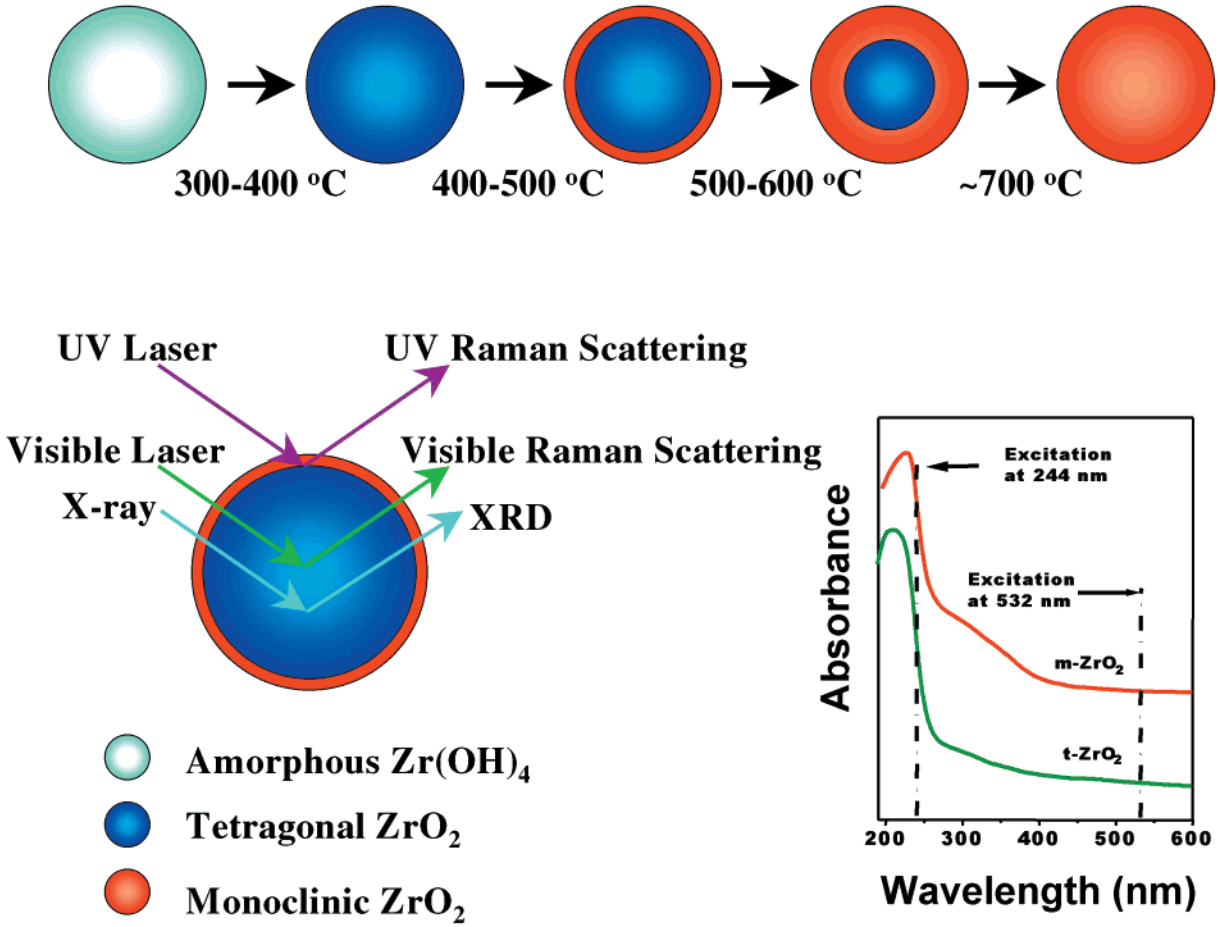

Figure 7. Schematic description of the phase evolution of zirconia calcined at different temperatures and the information obtained from UV Raman spectroscopy, visible Raman spectroscopy, and XRD. The inset is the UV−visible absorbance of m-ZrO_2 and t-ZrO_2.

From the comparison between Figure 1 and Figure 5, it is clearly seen that there are distinct differences in UV Raman spectra between the unpressed and pressed powder samples. In the spectra of the unpressed powder sample, the Raman bands due to both t-ZrO_2 and m-ZrO_2 are equally observed for the sample calcined at 400 °C. However, for the pressed sample calcined at 400 °C, Raman spectrum indicated that the zirconia is nearly all in t-ZrO_2 phase. As the calcination temperature was increased to 500 °C, only the Raman bands of m-ZrO_2 are observed for the unpressssed powder sample (Figure 1), but the Raman bands of t-ZrO_2 are still strong for the pressed sample (Figure 5). This suggests that the t-ZrO_2 phase is more stable for the pressed sample, and its phase change from tetragonal to monoclinic is obviously retarded.

The difference between unpressed and pressed samples can be seen in XRD patterns in Figure 2 and Figure 6. After the unpressed sample was calcined at 400 °C, the diffraction peaks of t-ZrO_2 are dominant, but with relatively weak peaks of m-ZrO_2 (Figure 2), while only the diffraction peaks of t-ZrO_2 are observed for pressed sample (Figure 6**)**. When the unpressed sample was calcined at 500 °C, the diffraction peaks of both of t-ZrO_2 and m-ZrO_2 are detected with equal intensities (Figure 2); but the diffraction peaks are due to t-ZrO_2 phase are mainly observed for the pressed sample calcined at 500 °C (Figure 6).

On the basis of the results presented above, it can be concluded that t-ZrO_2 phase is more stable after the powder of ZrO_2 sample was pressed before its calcination. It turns out that pressing the sample will retard the transformation from the tetragonal phase to the monoclinic phase. This can be interpreted as that the sample pressing may induce the particle agglomeration of amorphous zirconium hydroxide. The agglomerated particle may experience a slower phase transformation than smaller particles. It was reported that a slow addition of base during the precipitation process led to the polymerization of zirconia, that makes the t-ZrO_2 stable.[31] These results indicated that the agglomerated bigger particle of amorphous zirconium hydroxide is beneficial to the formation and stabilization of t-ZrO_2 phase.

A schematic description of the phase transformation of zirconia as deduced from UV Raman spectra, visible Raman spectra and XRD is shown in Figure 7. When the samples are excited by a UV laser, e.g., 244-nm laser light, the Raman signals are mostly from the surface region of ZrO_2 because ZrO_2 absorbs both the excitation laser and the scattering light in the UV region. As a result, only the scattering light from the surface region can escape from the absorption. The phase transformation is actually a process from the surface region to the bulk of ZrO_2, namely, the monoclinic phase is initially formed at the surface region of the tetragonal zirconia particle. Although m-ZrO_2 is a thermodynamically more stable phase, owing to kinetic effect, the transformation from t-ZrO_2 to m-ZrO_2 is a slow process from the surface region to the bulk as shown in Figure 7. As the particle size is reduced, the phase transformation from t-ZrO_2 to m-ZrO_2 is easier because the portion of the surface region in the whole particle is increased. This explains the phenomenon that the t-ZrO_2 phase can be stable to higher temperatures for the agglomerated particle. Figure 7 also gives a visual illustration for the different information obtained from UV Raman spectroscopy, visible Raman spectroscopy, and XRD, and among them the UV Raman spectroscopy is more surface sensitive.

Conclusion

Tetragonal zirconia (t-ZrO_2) begins to change into monoclinic zirconia (m-ZrO_2) when the calcination temperature is increased to 400 °C. It is found that UV Raman spectroscopy is more surface-sensitive than XRD and visible Raman spectroscopy for ZrO_2 because zirconia absorbs UV light. The m-ZrO_2 phase is detected by UV Raman spectroscopy for the samples calcined at lower temperatures than when it is detected by XRD or visible Raman spectroscopy. The results of UV Raman spectroscopy, visible Raman spectroscopy, and XRD suggest that the phase transformation of ZrO_2 from tetragonal to monoclinic takes place initially at the surface regions of ZrO_2 particle. Agglomeration of amorphous zirconium hydroxide particle favors stabilization of t-ZrO_2, because the portion of surface region in the whole particle is decreased when the particle size is increased.

Acknowledgment. This work was financially supported by the State Key Project (Grant 19999022407) of the Ministry of Science and Technology, People's Republic of China, and the National Science Foundation of China(NSFC) for Distinguished Young Scholars (Grant 29625305).

References and Notes

(1) Srinivasan, R.; Davis, B. H. *Catal. Lett.* **1992**, *14*, 165.

(2) Stefanic, G.; Music, S.; Grzeta, B.; Popovic, S.; Sekulic, A. *J. Phys. Chem. Solids* **1998**, *59*, 879.

(3) Xia, B.; Duan, L.-Y.; Xie, Y.-CH. *J. Am. Ceram. Soc.* **2000**, *83* (5), 1077−1080.

(4) Su, S. C.; Bell, A. T. *J. Phys. Chem.* B **1998**, *102*, 7000.

(5) Dang, Z.; Anderson, B. G.; Amenomiya, Y.; Morrow, B. A. *J. Phys. Chem.* **1995**, *99*, 14437.

(6) Miller, J. M.; Lakshmi, L. J. *J. Phys. Chem. B* **1995**, *102*, 6465.

(7) Tanabe, K. *Mater. Chem. Phys.* **1985**, *13*, 347.

(8) Srinivasan, R.; Taulbee, D.; Davis, B. H. *Catal. Lett.* **1991**, *9*, 1.

(9) Tanabe, K.; Misono, M.; Ono, Y.; Hattori, H. *Stud. Surf. Sci. Catal.* **1989**, *51*, 1.

(10) Hino, M.; Kobayashi, S.; Arata, K. *J. Am. Chem. Soc.* **1979**, *101*, 6439.

(11) Davis, B. H.; Keogh, R. A.; Srinivasan, R. *Catal. Today* **1994**, *20*, 219.

(12) Morterra, C.; Bolis, V.; Cerrato, G.; Magnacca, G. *Surf. Sci.* **1994**, *304*, 1206.

(13) Morterra, C.; Bolis, V.; Cerrato, G.; Pinna, F.; Signoretto, M. *J. Phys. Chem.* **1994**, *98*, 12373.

(14) Pacheco, G.; Fripiant, J. J. *J. Phys. Chem. B* **2000**, *104*, 11906.

(15) Stefanic, I. I.; Music, S.; Stefanic, G.; Gajovic, A. *J. Mol. Struct.* **1999**, *480*−*481*, 621.

(16) Comelli, R. A.; Vera, C. R.; Parera, J. M. *J. Catal.* **1995**, *151*, 96.

(17) Sekkulic, A.; Furic, K. *J. Mater. Sci. Lett.* **1997**, *16*, 260.

(18) Hirata, T.; Asari, E.; Kitajima M. *J. Solid State Chem.* **1994**, *110*, 201.

(19) Garvie, R. C. *J. Phys. Chem.* **1965**, *69*, 1238.

(20) Djurado, E.; Bouvier, P.; Lucazeau, G. *J. Solid State Chem.* **2000**, *149*, 399.

(21) Murase, Y.; Kato, E. *J. Am. Ceram. Soc.* **1982**, *66*, 196.

(22) Mirgordsky, A. P.; Smirnor, M. B.; Quintard, P. E. *Phys. Rev. B* **1997**, *55*, 19.

(23) Neigita, K.; Takao, H. *J. Phys. Chem. Solids* **1989**, *50*, 325.

(24) Stair, P. C.; Li, C. *J. Vac. Sci. Technol. A* **1997**, *15*, 1679.

(25) Xiong, G.; Li, C.; Feng, Z.; Ying, P.; Xin, Q.; Liu, J. *J. Catal.* **1999**, *186*, 234.

(26) Li, C.; Stair, P. C. *Stud. Surf. Sci. Catal.* **1997**, *105*, 599.

(27) Li, C.; Xiong, G.; Xin, Q.; Liu, J.; Ying, P.; Feng, Z.; Li, J.; Yang, W.; Wang, Y.; Wang, G.; Liu, X.; Lin, M.; Wang, X.; Min, E. *Angew. Chem., Int. Ed.* **1999**, *38*, 2220.

(28) Li, C.; Stair, P. C. *Catal. Lett.* **1996**, *36*, 119.

(29) Hu, Y.-H.; Dong, L.; Wang, J.; Chen, Y.; Li, C.; Li, M.-J.; Feng, ZH-CH.; Ying, P.-L. *Chem. Lett*. **2000,** 904.

(30) Shi, L.; Tin, K.; Wong, N. *J. Mater. Sci.* **1999**, *34*, 3367.

(31) Cleatfield, A. J. *Mater. Res.* **1990**, *5*, 161